

Liquid Crystalline Polyethers Based on Conformational Isomerism. 15.[†] Smectic and Crystalline Phases in Copolyethers Based on 1,2-Bis(4-hydroxyphenyl)ethane and Combinations of 1,10-Dibromodecane with 1,12-Dibromododecane and of 1,8-Dibromooctane with 1,12-Dibromododecane

G. Ungar*

School of Materials, The University of Sheffield, Sheffield, S10 2TZ, U.K.

J. L. Feijoo

H. H. Wills Physics Laboratory, The University of Bristol, Bristol BS8 1TL, U.K.

V. Percec* and R. Yourd

Department of Macromolecular Science, Case Western Reserve University, Cleveland, Ohio 44106

Received May 23, 1990; Revised Manuscript Received August 30, 1990

ABSTRACT: The synthesis and characterization of copolyethers based on 1,2-bis(4-hydroxyphenyl)ethane (BPE) and a 1/1 molar ratio of 1,10-dibromodecane with 1,12-dibromododecane [BPE-10/12(1/1)] and, respectively, BPE and a 1/1 molar ratio of 1,8-dibromooctane with 1,12-dibromododecane [BPE-8/12(1/1)] are described. A combination of techniques consisting of differential scanning calorimetry (DSC), simultaneous X-ray diffraction/DSC (XDDSC), and thermal optical polarized microscopy was used for the characterization of both copolymers. BPE-10/12(1/1) exhibits two orthorhombic crystalline (Cr and Cr') phases and an enantiotropic smectic B phase (probably the crystal B variant). In the Cr phase the spacers are crystalline, while in the Cr' phase they are in a molten state. BPE-8/12(1/1) exhibits an enantiotropic smectic B phase and an enantiotropic hexagonal columnar mesophase. Fibers drawn from BPE-10/12(1/1) orient the plane of the smectic layer parallel to the draw direction, suggesting that a substantial fraction of polymer chains form reentrant folds within the spacer layer. This result is contrary to findings in previous main-chain liquid crystalline polymers where the plane of the smectic layer aligns perpendicular to the draw direction.

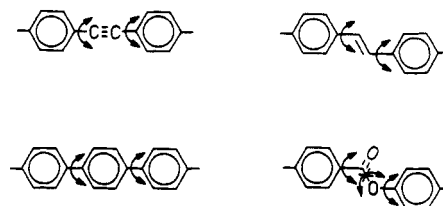
Introduction

In the previous publications from this series we have advanced the concept of flexible rodlike mesogenic unit or rodlike mesogenic unit based on conformational isomerism. This concept was already used to synthesize main-chain liquid crystalline polyethers based on conformational isomerism without,¹ and with,²⁻¹³ flexible spacers. While in the case of rigid rodlike mesogenic units the rodlike conformation is created and maintained through the conformational rigidity of the molecule,¹⁴⁻¹⁷ in the case of rodlike mesogenic units based on conformational isomerism, the rodlike conformation is created and maintained through thermodynamics¹⁻⁹ (Scheme I).

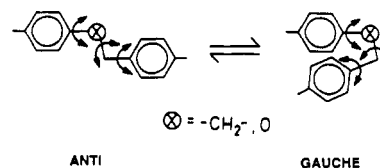
So far, we have reported the synthesis and characterization of homopolyethers and binary copolyethers based on 1-(4-hydroxyphenyl)-2-(2-methyl-4-hydroxyphenyl)ethane (MBPE) and α,ω -dibromoalkanes containing from 4 to 20 methylene units in their flexible spacer.²⁻¹³ Copolyethers based on MBPE and three⁶ or more than three¹² flexible spacers were also investigated. All these polyethers display virtual, monotropic, or enantiotropic nematic mesophases.²⁻²⁰ The transformation of virtual or monotropic mesophases of homopolymers into enantiotropic mesophases can be accomplished by copolymerization. We have demonstrated that copolymerization not only transforms virtual and monotropic mesophases into enantiotropic mesophases but also leads to the only available technique to determine the thermal transition temperatures and thermodynamic parameters of virtual

Scheme I Comparison of Rigid and Flexible Rodlike Mesogens or Rodlike Mesogens Based on Conformational Isomerism

Rigid Rod-like Mesogens



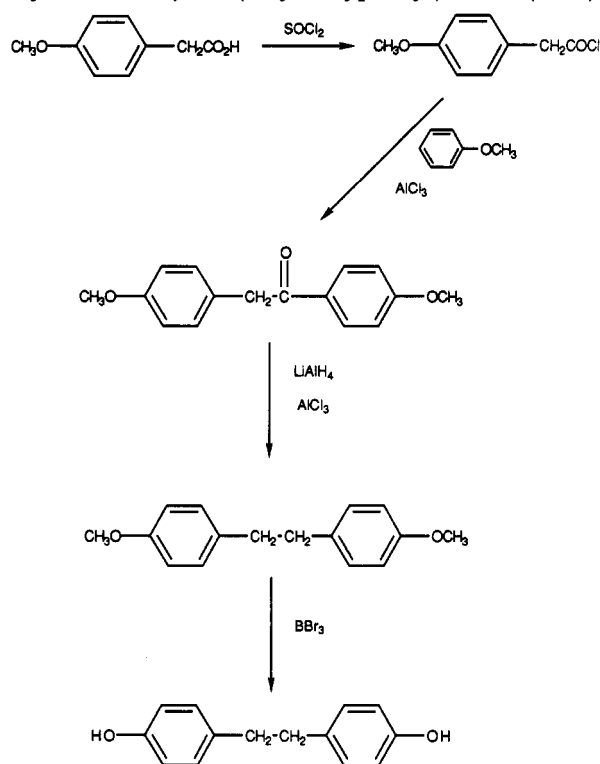
Flexible Rod-like Mesogens or Rod-like Mesogens Based on Conformational Isomerism



mesophases displayed by homopolymers.²⁻¹³ Although blends of two or more than two polymers displaying virtual mesophases can be used for the same purpose, this last technique is much less powerful than copolymerization.²⁻¹³ Simultaneous X-ray diffraction/DSC experiments were used to demonstrate that the mesophases displayed by these polymers and copolymers are uniaxial nematic.¹⁸

[†] Part 14 in this series: Reference 18.

Scheme II Synthesis of 1,2-Bis(4-hydroxyphenyl)ethane (BPE)



The goal of this paper is to describe the synthesis and characterization of the first examples of liquid crystalline polyethers based on conformational isomerism that exhibit smectic mesomorphism. The particular examples to be described here refer to copolyethers based on 1,2-bis(4-hydroxyphenyl)ethane (BPE) and a 1/1 molar ratio of 1,10-dibromodecane with 1,12-dibromododecane [BPE-10/12(1/1)] and, respectively, BPE and a 1/1 molar ratio of 1,8-dibromooctane with 1,12-dibromododecane [BPE-8/12(1/1)].

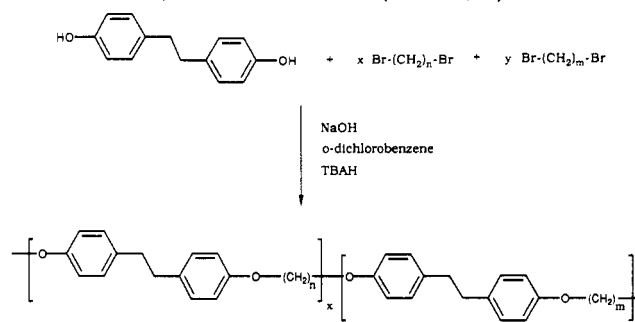
Experimental Section

Materials. Boron tribromide (1.0 M in CH_2Cl_2), 1,10-dibromodecane (97%), 1,8-dibromooctane (98%), lithium aluminum hydride (99%), thionyl chloride (97%), Aliquat 336 (trimethylcaprylammonium bromide), *o*-dichlorobenzene (99%) (all from Aldrich), and (4-methoxyphenyl)acetic acid (99%, Lancaster Synthesis) were used as received. 1,12-Dibromododecane (technical, Aldrich) was recrystallized once from methanol. Chloroform and methylene chloride were dried over calcium hydride, followed by distillation. Diethyl ether was dried over LiAlH_4 and then distilled.

Scheme II describes the synthesis of 1,2-bis(4-hydroxyphenyl)ethane (BPE).

Synthesis of 1,2-Bis(4-methoxyphenyl)ethanone (Desoxy-anisoin). Thionyl chloride (42.96 g, 0.362 mol) was added dropwise to a mixture of 40.0 g (0.240 mol) of (4-methoxyphenyl)acetic acid in 200 mL of dry methylene chloride. The resulting mixture was refluxed for 2 h, after which the excess thionyl chloride and methylene chloride were removed by distillation under reduced pressure. The resulting acid chloride was used directly in the acylation reaction. (4-Methoxyphenyl)acetyl chloride (44.44 g, 0.240 mol) and anisole (53.24 g, 0.492 mol) were dissolved in 400 mL of dry methylene chloride. The resulting solution was cooled to below 10 °C in an ice water bath, after which 49.38 g (0.370 mol) of anhydrous AlCl_3 was added slowly and in small portions so that the reaction temperature did not rise above 15 °C. After all the AlCl_3 was added, the ice bath was removed and the solution was stirred at room temperature for 15 min. The reaction mixture was then poured into a mixture of 100 mL of HCl and 400 mL

Scheme III Synthesis of Polyethers and Copolyethers Based on 1,2-Bis(4-hydroxyphenyl)ethane (BPE) and α,ω -Dibromoalkanes (BPE-X/Y)



of ice water. The organic layer was separated and washed sequentially with H_2O , 10% aqueous NaOH, and H_2O , after which it was dried with MgSO_4 and filtered and the methylene chloride was removed on a rotary evaporator. The crude product was recrystallized twice from ethanol to give 46.6 g (75.8%) of white needlelike crystals. Mp (DSC, 20 °C/min): 111 °C. ^1H NMR (CDCl_3 , TMS): δ 3.74 (3 protons, $-\text{OCH}_3$ of the phenyl ring attached to the methylene group, s), 3.81 (3 protons, $-\text{OCH}_3$ of the phenyl ring attached to the carbonyl group, s), 4.14 (2 protons, $-\text{CH}_2\text{CO}-$, s), 6.84 (2 protons, ortho to methoxy on the phenyl ring attached to the carbonyl group, d), 6.89 (2 protons, ortho to methoxy on the phenyl ring attached to the methylene group, d), 7.17 (2 protons, meta to methoxy on the phenyl ring attached to the methylene group, d), 7.97 (2 protons, meta to methoxy on the phenyl ring attached to the carbonyl group, d).

Synthesis of 1,2-Bis(4-methoxyphenyl)ethane. AlCl_3 (31.68 g, 0.238 mol) was added slowly to 140 mL of dry diethyl ether, and the resulting solution was added dropwise to a slurry of LiAlH_4 (4.1 g, 0.108 mol) in dry diethyl ether under nitrogen atmosphere. To this reducing agent² was added dropwise a solution of desoxyanisoin (11.23 g, 0.0438 mol) in 75 mL of dry chloroform. The resulting suspension was stirred for 3 h at room temperature. A mixture of 115 mL of HCl and 150 mL of distilled water was then carefully added to the reaction mixture. The ether layer was separated and washed three times with distilled water. After drying with anhydrous magnesium sulfate, the solution was filtered and the solvent was removed on a rotary evaporator. The crude product was recrystallized from 700 mL of 95% ethanol to give 5.0 g of white needlelike crystals. Mp: 125–127 °C. Subsequent concentration and crystallization of the filtrate yielded 4.0 g more of the product for a total yield of 9.0 g (84.7%). ^1H NMR showed both crystal fractions to be essentially 100% pure with no evidence of unreduced carbonyl. ^1H NMR ($\text{DMSO}-d_6$): δ 2.76 (4 protons, $-\text{CH}_2\text{CH}_2-$, s), 3.70 (6 protons, $-\text{OCH}_3$, s), 6.81 (4 protons, ortho to methoxy on the phenyl ring, d), 7.10 (4 protons, meta to methoxy on the phenyl ring, d).

Synthesis of 1,2-Bis(4-hydroxyphenyl)ethane. A solution of 1,2-bis(4-methoxyphenyl)ethane (8.4 g, 0.0347 mol) in 150 mL of dry methylene chloride was added dropwise under dry nitrogen atmosphere to 80 mL (0.078 mol) of 1.0 M BBr_3 in methylene chloride cooled in a dry ice/acetone bath. After the mixture was stirred at room temperature overnight, enough H_2O was added to hydrolyze the excess BBr_3 . Ether was added to dissolve the solid that had formed. The ether layer was separated and washed three times with H_2O . The solution was then dried with anhydrous magnesium sulfate, and the solvent was removed on a rotary evaporator. The resulting white solid was recrystallized from 100 mL of 1/1 ethanol/ H_2O . Purity (HPLC): 100%. Mp (DSC, 20 °C/min): 200 °C. ^1H NMR ($\text{DMSO}-d_6$): δ 2.69 (4 protons, $-\text{CH}_2\text{CH}_2-$, s), 6.66 (4 protons, ortho to hydroxy on the phenyl ring, d), 6.97 (4 protons, meta to hydroxy on the phenyl ring, d).

Synthesis of Polyethers and Copolyethers. Synthesis of polyethers and copolyethers based on 1,2-bis(4-hydroxyphenyl)ethane (BPE) and α,ω -dibromoalkanes is outlined in Scheme III. Conventional liquid-liquid two-phase (organic solvent/aqueous NaOH solution) phase-transfer-catalyzed polyetherification conditions were used for the preparation of the polyethers

Table I
Characterization of Copolyethers Based on BPE and 1,8-Dibromooctane, 1,10-Dibromodecane, and 1,12-Dibromododecane

copolymer BPE- <i>X</i> / <i>Y</i> (<i>A</i> / <i>B</i>)	yield, %	M_n	M_w/M_n	thermal transitions (°C) and corresponding enthalpy changes (kcal/mru) in parentheses ^a	
BPE-10/12(1/1)	93.5	14 400	2.40	1st heating scan	k156s172(5.91*)i
				2nd heating scan	k145k154s171(8.19*)i
				2nd cooling scan	i157(7.96*)s142k136k
BPE-8/12(1/1)	90.3	23 300	2.4	1st heating scan	s104(0.52)h _c 181(4.58)i
				2nd heating scan	s111(0.10)h _c 180(4.66)i
				2nd cooling scan	i166(4.39)h _c 86(0.14)s

^a Asterisk indicates enthalpy changes that correspond to overlapped transition peaks.

and copolyethers. The polyetherifications were carried out under nitrogen atmosphere at 80 °C in an *o*-dichlorobenzene/10 N NaOH water solution (10 times molar excess of NaOH versus phenol groups) in the presence of Aliquat 336 (10 mol % of phenol groups) as phase-transfer catalyst. The ratio of electrophilic to nucleophilic monomers was in every case 1.0/1.0.

The synthesis of the copolyether based on BPE and a 1/1 molar ratio of 1,10-dibromodecane to 1,12-dibromododecane is detailed below as an example of copolyetherification. To a 25-mL single-neck flask equipped with condenser and nitrogen inlet-outlet were successively added 0.2500 g (1.1668 mmol) of BPE, 2.3 mL of 10 N NaOH, 0.1750 g (0.5834 mmol) of 1,10-dibromodecane, 0.1914 g (0.5834 mmol) of 1,12-dibromododecane, 0.1914 g (0.5834 mmol) of 1,12-dibromododecane, 2.0 mL of *o*-dichlorobenzene, and 0.0943 g (0.2334 mmol) of Aliquat 336. The reaction mixture was stirred at 1100 rpm with a magnetic stirrer at 80 °C under nitrogen. After 6 h of reaction, 5 mL of chloroform was added to the reaction mixture, followed by 10 mL of water to separate the two phases. The aqueous layer was removed, and the organic phase was washed several times with water, followed by dilute hydrochloric acid, and finally with water again. The polymer was separated by precipitation of the polymer solution into methanol to obtain 0.3999 g (93.5%) of a white, fibrous precipitate. The polymer was further purified by two subsequent precipitations from chloroform solutions into acetone and then into methanol.

In this entire paper the polyethers will be designated BPE-*X* where *X* is the number of methylene units in the spacer. Similarly, copolyethers will be designated BPE-*X*/*Y*(*A*/*B*) where *X* is the number of methylene units in one of the spacers, *Y* is the number of methylene units in the other, and *A*/*B* refers to the molar ratio of the two spacers.

Techniques. ¹H NMR (200-MHz) spectra were recorded on a Varian XL-200 spectrometer.

Molecular weights were determined by gel permeation chromatography (GPC). High-pressure liquid chromatography (HPLC) and GPC analyses were carried out with a Perkin-Elmer Series 10LC equipped with a LC-100 column oven, LC 600 autosampler, and a Sigma 15 data station. The measurements were made by using the UV detector, tetrahydrofuran as solvent (1 mL/min, 40 °C), a set of PL gel columns of 10², 5 × 10², 10³, 10⁴, and 10⁵ Å, and a calibration plot constructed with polystyrene standards.

A Perkin-Elmer DSC-4 differential scanning calorimeter equipped with a TADS data station Model 3600 was used to determine the thermal transitions. Heating and cooling rates were 20 °C/min in all cases unless stated. First-order transitions were read at the maximum of the endothermic or exothermic peaks. The transitions reported were taken from the second or third heating or cooling scans.

A Carl Zeiss optical polarizing microscope equipped with a Mettler FP-82 hot stage and a Mettler 800 central processor was used to observe the thermal transitions and to analyze the textures.^{19,20}

Simultaneous X-ray diffraction and differential scanning calorimetry (XDDSC) experiments were performed with an experimental setup that was described in a previous publication.²¹ In this method, time-resolved powder diffractograms are collected during linear heating or cooling of the specimen, while at the same time the differential heat flow in or out of the specimen is recorded. Thus diffractograms can be unambiguously related to the features (peaks) in the thermogram, and transient metastable

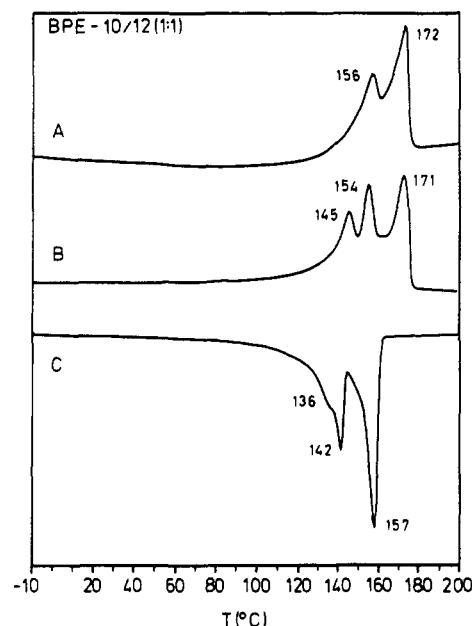


Figure 1. Representative heating and cooling DSC traces (20 °C/min) of BPE-10/12(1/1): (A) first heating scan; (B) second and subsequent heating scans; (C) first and subsequent cooling scans.

phases, as well as those existing in a narrow temperature range, can be easily identified.^{18,21} The powerful X-ray beam was provided by the synchrotron source at Daresbury, U.K. The technique has originally been introduced by Russel and Koberstein,²² and the details of our improved version are presented elsewhere.²¹

X-ray scattering patterns were recorded by using a flat-plate wide-angle (WAXS) vacuum camera (room temperature and elevated temperatures). Ni-filtered CuK α radiation was used. The samples were in the form of (a) fibers pulled from the melt, (b) bulk samples in Lindemann capillaries cooled from the melt, or (c) as-prepared polymers in the form of a free-standing powder. The temperature stability of the X-ray cell was ± 0.1 °C.

Results and Discussion

Table I summarizes the characterization of BPE-10/12(1/1) and BPE-8/12(1/1). The synthesis and characterization of the parent homopolymers BPE-8, BPE-10, and BPE-12 as well as of their copolyethers with different compositions will be described in another publication. On the first heating scan BPE-10/12(1/1) exhibits two endotherms at 156 and 172 °C (Figure 1A). The endotherm at 156 °C corresponds to a melting into a smectic phase that undergoes isotropization at 172 °C. On the cooling DSC scans BPE-10/12(1/1) exhibits three exotherms at 157, 142, and 136 °C (Figure 1C). From 157 to 142 °C BPE-10/12(1/1) exhibits a smectic phase that crystallizes at 142 °C. Second and subsequent heating scans display two melting transitions at 145 and 154 °C, followed by the smectic mesophase that undergoes isotropization at 171 °C. The assignment of the crystalline and smectic phases

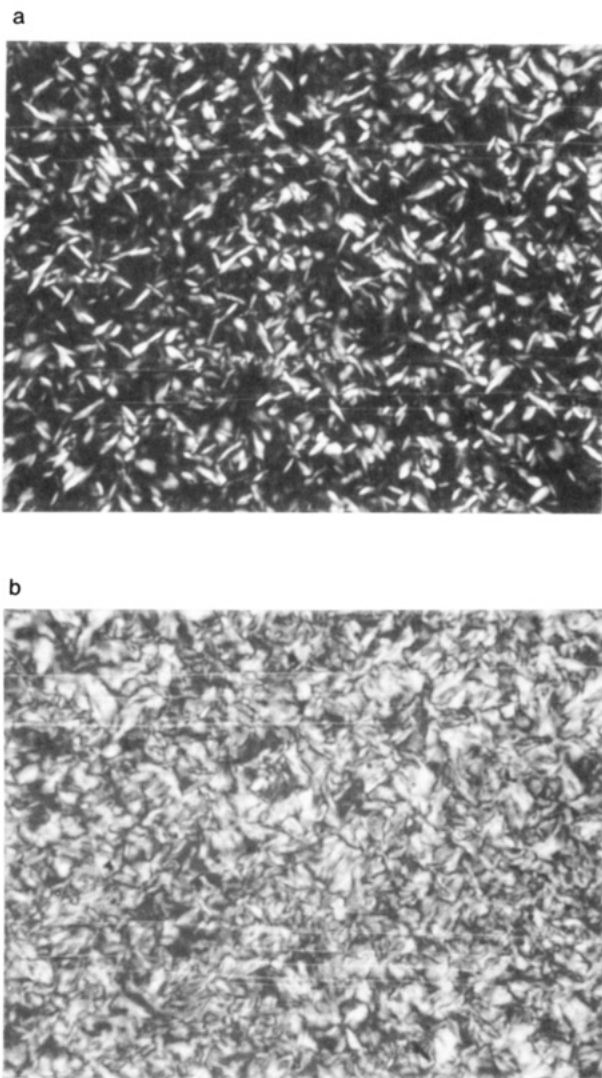


Figure 2. Optical polarized micrographs (75 \times) of the smectic phase of BPE-10/12(1/1): (a) batonnets at 165 $^{\circ}\text{C}$; (b) focal conic at 160 $^{\circ}\text{C}$.

was made by X-ray experiment, which will be discussed in the second part of this paper. On cooling from the isotropic phase, the smectic phase of BPE-10/12(1/1) appears first as batonnets (Figure 2a), which upon annealing transform into a focal-conic texture (Figure 2b).

Figure 3 presents representative DSC traces of BPE-8/12(1/1). This copolymer does not crystallize. Below 104 $^{\circ}\text{C}$ on the first heating scan (Figure 3A) or 111 $^{\circ}\text{C}$ on the second heating scan (Figure 3B), BPE-8/12(1/1) presents a smectic mesophase. From 104 to 181 $^{\circ}\text{C}$ on the first heating scan and from 111 to 180 $^{\circ}\text{C}$ on the second heating scan this copolymer exhibits a hexagonal columnar mesophase. Both the smectic and the columnar mesophase of BPE-8/12(1/1) are enantiotropic (Figure 3). The smectic mesophase will be characterized in this paper. However, the characterization of the hexagonal columnar mesophase will be presented in a subsequent publication.

Figure 4a shows the extended conformation of a BPE-10 dimer. The $-\text{O}(\text{CH}_2)_{10}-$ spacer is in the all-trans conformation. The molecular parameters of the diphenylethane unit are taken from the crystallographic data on dibenzyl.²³ The monomer repeat distance in this model is 25.2 \AA . While this conformation has the minimum energy in the case of an isolated chain, the work of Bryan et al.^{25,26} on *p*-alkoxybenzoic acids indicated that in the crystalline and smectic states the preferred conformation

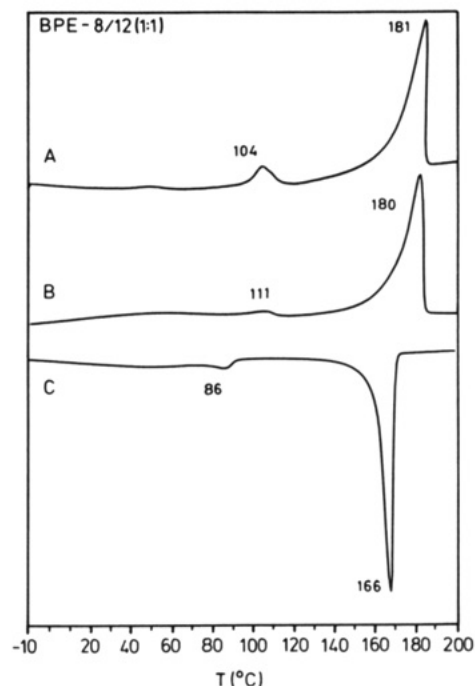


Figure 3. Representative heating and cooling DSC traces (20 $^{\circ}\text{C}/\text{min}$) of BPE-8/12(1/1): (A) first heating scan; (B) second and subsequent heating scans; (C) first and subsequent cooling scans.

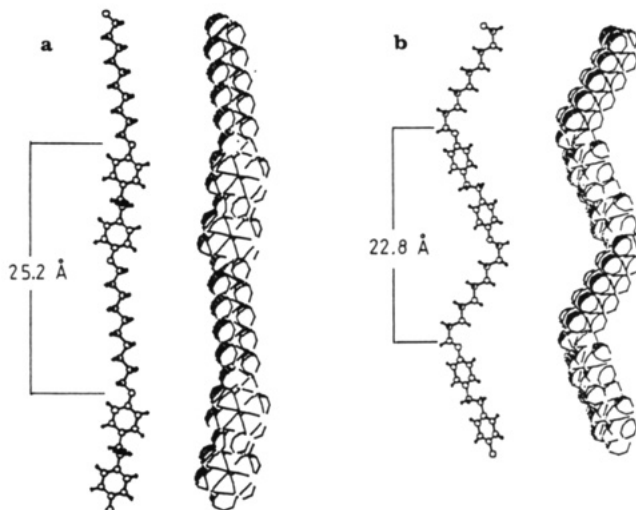


Figure 4. (a) Molecular models of a BPE-10 dimer unit in the extended conformation (all bonds within the alkylene spacers are trans). (b) Molecular models of a BPE-10 dimer unit in the "crimped" conformation (end C-C bonds in the alkylene spacers are gauche).

is one where, in the alkylene moiety, the $\text{C}^{\alpha}-\text{C}^{\beta}$ bond adjacent to the ether oxygen is gauche. The model of the BPE-10 chain with two opposite gauche bonds next to the ether groups, i.e., $\text{C}^{\alpha}-\text{C}^{\beta}$ and $\text{C}^{\phi}-\text{C}^{\omega}$ bonds, is shown in Figure 4b. In this model the monomer repeat distance is 22.8 \AA .

X-ray investigations were carried out by using the simultaneous X-ray diffraction/DSC technique (XDDSC).²¹ Figure 5a presents the DSC thermogram recorded during a XDDSC cooling scan at 5 $^{\circ}\text{C}/\text{min}$, starting from the isotropic melt. The corresponding X-ray diffractograms, recorded every 24 s (every 2 $^{\circ}\text{C}$), are shown in Figure 5b. The diffractograms corresponding to the positions of the numbered arrows in the thermogram, i.e., to the two endothermic peaks and the shoulder, are emphasized in Figure 6.

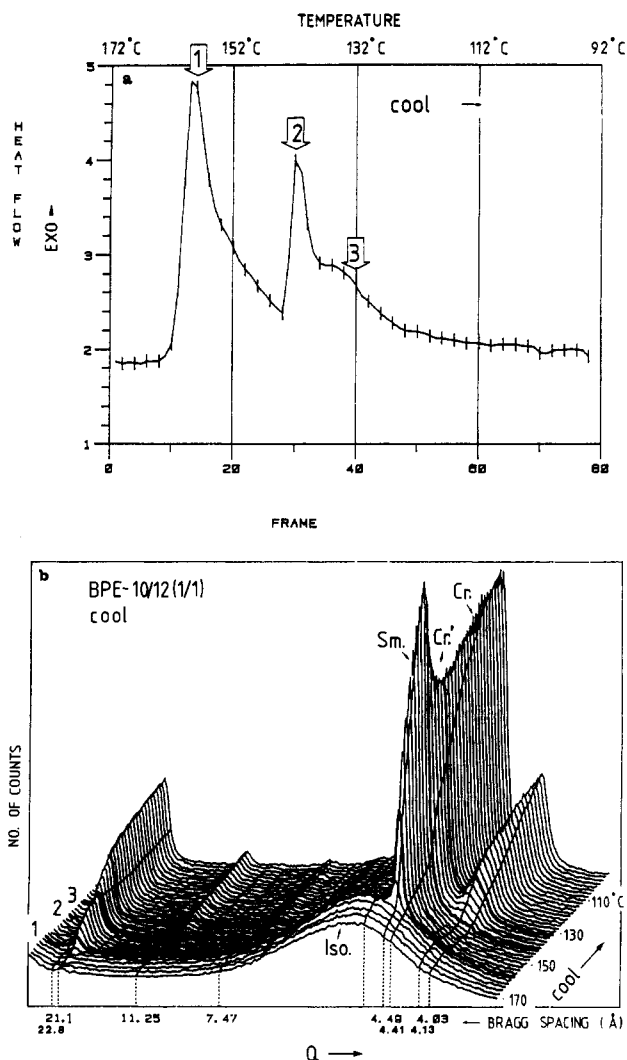


Figure 5. XDDSC cooling scan of the BPE-10/12(1/1) copolymer, spanning the isotropic (Iso), smectic (Sm), and two crystalline phases (Cr and Cr'). Cooling rate 5 °C/min. (a) DSC thermogram. (b) Simultaneously recorded diffractograms. The bold curves in Figure 5b correspond to the positions in the thermogram marked by the numbered arrows. Note that each curve in Figure 5b is an average of two 12-s time frames.

Four thermotropic phases are distinguished in BPE-10/12(1/1), three of which are shown as separate time-averaged diffraction curves in Figure 5: the isotropic melt (Iso) above 164 °C, the smectic phase (Sm) between the two strong exotherms, and the crystal phase (Cr) below 130 °C. The phase between 140 and 132 °C is a crystalline variant, denoted Cr' (Figure 5a,b).

All four phases in BPE-10/12(1/1) are enantiotropic, and the heating XDDSC scan is the almost exact reversal of the cooling scan (Figure 7).

The three wide-angle reflections of the crystalline phase below 130 °C can be easily indexed on an orthorhombic unit cell with $a = 9.46$ Å and $b = 4.41$ Å. The peaks at 4.72, 4.41, and 4.03 Å would thus be the 200, 010, and 110 reflections, respectively. The fact that all three reflections are $hk0$ suggests that chains are perpendicular to the layers. The projection down the chain axis of a unit cell compatible with the observed diffraction pattern is schematically shown in Figure 8. The two crystallographically nonequivalent chains are denoted as X and Y.

Note that the layer spacing (22.8 Å) in the crystalline phase matches exactly the monomer repeat of 22.8 Å in the second model of the BPE-10 molecule (Figure 4b). It is reasonable to expect that the average layer spacing would

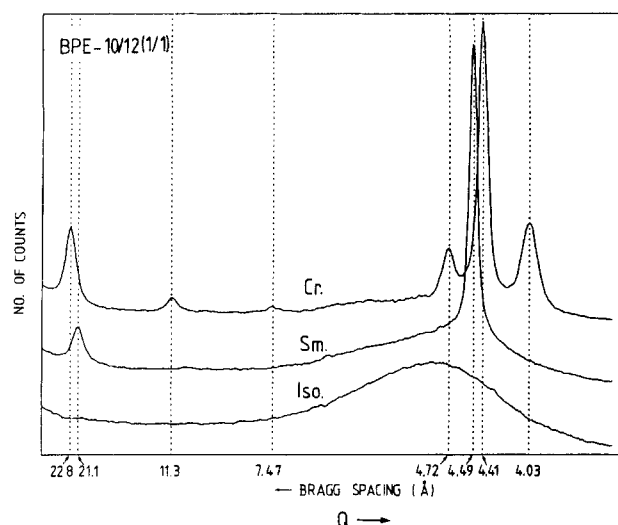


Figure 6. X-ray diffractograms of the three main phases in BPE-10/12(1/1): isotropic, smectic, and low-temperature crystalline.

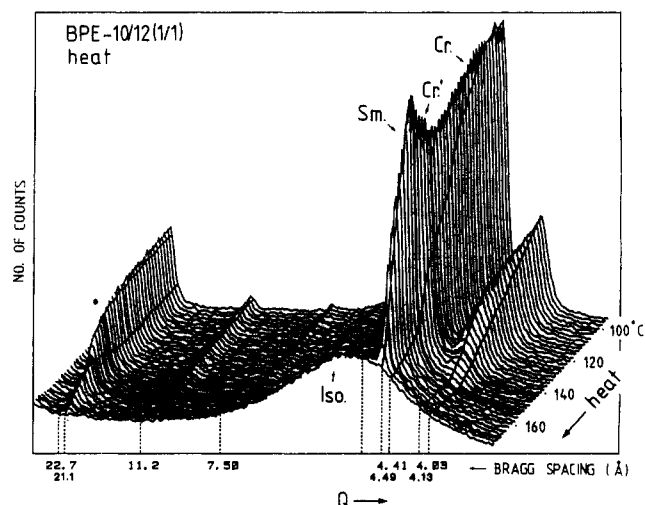


Figure 7. XDDSC heating scan of BPE-10/12(1/1) previously cooled at 5 °C/min. Heating rate 10 °C/min. Bold curves correspond to the positions of the three endothermic DSC peaks (thermogram not shown).

be, in the main chain, governed by the length of the shorter spacer, and hence we do not expect the spacing in BPE-10/12(1/1) to be very different from that in the BPE-10 homopolymer. This decisive role of the shorter spacer has already been established in the case of layered crystals of copolyethers based on 4,4'-dihydroxy- α -methylstilbene and α,ω -dibromoalkanes.²⁷

The high-temperature crystalline phase, denoted Cr' in Figures 5b and 7, retains all the reflections of the low-temperature form, as far as can be established from the present powder diffractograms. In the wide-angle region, the 010 peak is slightly more intense, while the 200 and the 110 peaks are less intense, compared to the low-temperature Cr phase. The lateral cell dimensions are increased a little in the Cr' phase. The 001 layer reflections are somewhat unclear, and the layer spacing is by 0.5 Å smaller in the Cr' phase ($L_{Cr} = 22.8$ Å, $L_{Cr'} = 22.3$ Å). These selectively minor differences in the diffractograms are in contrast with the considerable difference in enthalpies of the Cr and Cr' phases. The Cr-Cr' transition enthalpy of 8.4 cal/g (entropy 7.2 cal/K·mru) is of the same order of magnitude as the enthalpy of the Cr-Sm transition measured as 6.2 cal/g (entropy 5.3 cal/K·mru). Note that the somewhat arbitrary separation of areas of

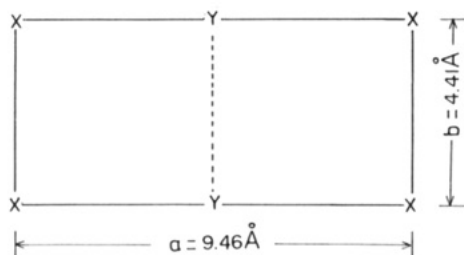


Figure 8. Projection down the chain axis of a unit cell of the crystalline phase of BPE-10/12(1/1) compatible with the observed diffraction pattern (schematic). The two crystallographically nonequivalent chains are denoted as X and Y.

the partially overlapping Cr–Cr' and Cr'–Sm peaks leads to an estimated 10% error in the above values.

There is little doubt that the orthorhombic unit cell of the Cr phase, with its cross section $a \times b = 9.46 \times 4.41 = 41.72 \text{ Å}^2$, contains two polymer chains. Thus the chain cross section is 20.86 Å, which is in the usual range for polymers of similar constitution.^{27–31} It is noted that this chain packing is fairly dense. Referring to the packing of alkylene parts, the cross section of 20.86 Å², or less if the alkylene chains are tilted (Figure 4b), is small enough for considerable interchain interaction. Similar cross section is found in the "rotator" phase of *n*-alkanes (19–20.5 Å²),³² and in the conformationally disordered hexagonal phase of polyethylene, when the value is extrapolated to atmospheric pressure (21–22.5 Å²).³³ If the alkylene spacers are in a similar partially ordered crystalline state in the Cr phase, it is quite possible that the Cr–Cr' transition involved "melting" of these spacers. If the entire entropy of the Cr–Cr' transition was apportioned among the 11 CH₂ groups of the average spacer, it would amount to 0.72 cal/K·mol of CH₂. This is of the same order as the entropy of the hexagonal–isotropic phase transition in polyethylene at atmospheric pressure estimated to be about 1.0 cal/K·mol of CH₂. Thus, in summary, the following three observations are consistent with melting of spacers in the Cr–Cr' transition: the Cr–Cr' transition is accompanied (a) by a small lateral unit cell expansion, (b) by a small contraction along the chain axis, and (c) by a considerable absorption of heat.

For comparison we note that, in a similar polymer, containing 4,4'-dihydroxy- α -methylstilbene mesogenic groups instead of BPE ones, the chain cross section was found to be 24.2 Å in the layered crystalline phase. This means that the alkylene layers in these polymers were already effectively "molten" in the crystalline phase. No phase change equivalent to the Cr–Cr' transition was observed in these polymers.²⁷

In addition to the 2 orders of layer reflections at low angles (21.1 and 10.5 Å), the smectic phase in BPE-10/12(1/1) also features a single intense wide-angle diffraction peak corresponding to a Bragg spacing of 4.49 Å. Thus the phase is of an ordered smectic type with a hexagonal arrangement of chains within the smectic layers. The wide-angle peak width is resolution limited, although the resolution of the position-sensitive detector used is relatively low. Thus we cannot be categorical, but it would appear that the phase is a crystal variant of an ordered smectic rather than a hexatic one.³⁵ The 4.49-Å smectic peak is actually sharper than the wide-angle reflections of the low-temperature crystalline phase in the preparation shown in Figure 5b.

It is not clear from the powder patterns whether chains are tilted or not in the smectic phase. We are inclined to believe that the reduction in layer spacing from 22.8 to 21.1 Å on the Cr–Sm transition is due to shrinkage of the

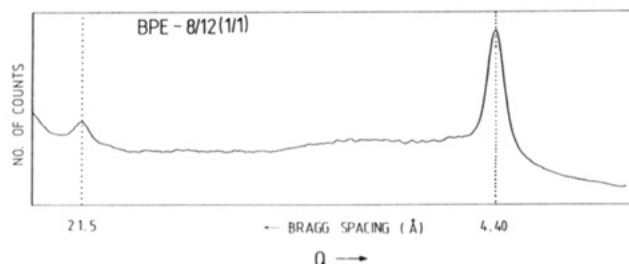


Figure 9. X-ray diffractogram of the smectic phase of BPE-8/12(1/1) recorded at 50 °C.

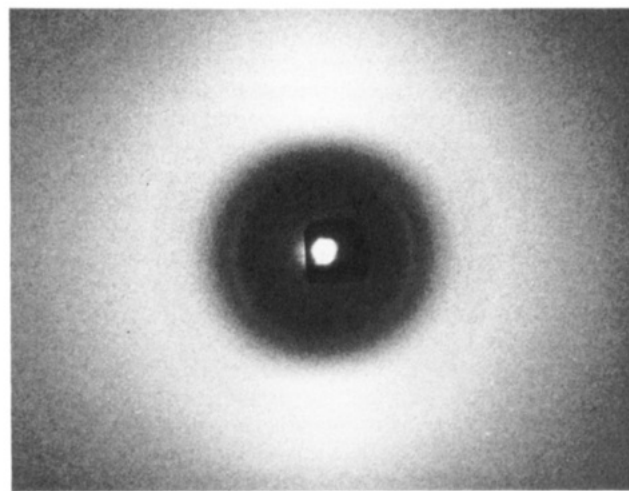


Figure 10. X-ray diffraction pattern showing the first-order layer reflection (two equatorial arcs) of the smectic phase of a melt-drawn fiber of BPE-10/12(1/1). Recorded at 150 °C with a flat-plate camera; Ni-filtered Cu K α radiation; fiber axis vertical.

chains through increased conformational disorder rather than tilting of whole chains. In tilted smectic phases like G and I other weaker reflections are usually observed around the main wide-angle diffraction peak, and these are not observed here. Thus it is likely that the "smectic" phase is of the crystal B type.³⁵ Note that the 4.49-Å spacing of the observed wide-angle reflection corresponds to a chain cross section of 23.3 Å² if the phase is crystal B. This cross section is sufficient for an essentially melt-like disorder of paraffin chains, but if the BPE molecule has a crimped conformation similar to that in Figure 4b, the alkylene spacers are tilted and the effective cross section is somewhat less.

Regarding the above discussion, it is interesting to compare the smectic phases in copolymer BPE-10/12(1/1) with that in BPE-8/12(1/1) (Figures 3 and 8). In the latter polymer there is a larger disparity in length of the two spacers (octylene versus dodecylene) and this greatly suppresses the crystalline melting point, so that the smectic phase is stable at room temperature (Figures 3 and 9). The diffractogram of the smectic phase of BPE-8/12(1/1) is similar to that of the smectic phase of BPE-10/12(1/1) (Figures 6 and 9). The smaller spacing of the wide-angle peak (4.40 versus 4.49 Å) is accounted for by the 100 °C difference in temperature of the recordings. However, it is interesting to note that, in spite of having shorter spacers, on average, the layer periodicity in BPE-8/12(1/1) is larger: 21.5 Å in BPE-8/12(1/1) versus 21.1 Å in BPE-10/12(1/1).

One possible explanation of the above apparent paradox in layer spacings is that the chains in BPE-8/12(1/1) are closer to the extended conformation (Figure 4a) than to the crimped one (Figure 4b). Since the octylene spacer is so much shorter than the dodecylene unit, the latter will

necessarily be contracted lengthwise and expanded laterally in order to approximately match the length of an extended octylene unit. This might require the full 23.3-Å² cross-sectional area per average chain and may therefore prohibit the tilt of alkylene chains, which would reduce this area. Thus, in BPE-8/12(1/1) an increased layer spacing would result. For example, the models of a chain of BPE-8 corresponding to those in parts a and b of Figure 4 give respective monomer repeat distances of 22.7 and 20.6 Å; these values are to be compared with the 21.5-Å spacing observed in BPE-8/12(1/1). The smectic phase of BPE-8/12(1/1) would appear to be of the B type.

Attempts have been made at producing oriented fibers by melt drawing. The copolymer BPE-10/12(1/1) was heated to the isotropic phase and stretched while cooled. Thus "solidification" occurred in the smectic state. The resulting orientation was poor, and fiber diffraction patterns did not provide further information about smectic or crystal structures. However, it is interesting that the smectic layers tended to align parallel to the draw direction (Figure 10). While this is the usual mode of orientation in smectic phases of low molar mass compounds and of side-chain polymers, where layers are free to slide past each other in the direction of shear, it is surprising that it is found in main-chain polymers. The usual mode of orientation in nematic^{8,36} and smectic,³⁷⁻³⁹ as well as crystalline, phases of melt-drawn main-chain polymers is one where the chains are parallel to the draw direction. Sliding of smectic layers is not easily visualized in BPE-X/Y(A/B) polymers, unless a substantial fraction of chains form reentrant folds within the spacer layers. This latter possibility is not to be excluded in the case of polymers with long spacers such as BPE-10/12(1/1).

The fact that the orientation achieved by melt drawing of BPE-10/12(1/1) was invariably poor may possibly be traced to the opposing and competing tendencies of both smectic layers and polymer chains to align parallel to the draw direction.

Acknowledgment. The financial support of this work by the National Science Foundation, Polymers Program (DMR-86-19724), is gratefully acknowledged.

References and Notes

- (1) Percec, V.; Yourd, R. *Macromolecules* **1988**, *21*, 3379.
- (2) Percec, V.; Yourd, R. *Macromolecules* **1989**, *22*, 524.
- (3) Percec, V.; Yourd, R. *Macromolecules* **1989**, *22*, 3229.
- (4) Percec, V.; Yourd, R. *Makromol. Chem.* **1990**, *191*, 25.
- (5) Percec, V.; Yourd, R. *Makromol. Chem.* **1990**, *191*, 49.
- (6) Percec, V.; Tsuda, Y. *Macromolecules* **1990**, *23*, 5.
- (7) Percec, V.; Tsuda, Y. *Polym. Bull.* **1989**, *22*, 489.
- (8) Percec, V.; Tsuda, Y. *Polym. Bull.* **1989**, *22*, 497.
- (9) Percec, V.; Tsuda, Y. *Polym. Bull.* **1990**, *23*, 225.
- (10) Percec, V.; Tsuda, Y. *Macromolecules* **1990**, *23*, 3509.
- (11) Percec, V.; Tsuda, Y. *Polymer*, in press.
- (12) Percec, V.; Tsuda, Y. *Polymer*, in press.
- (13) Percec, V.; Tsuda, Y. *Polym. Bull.* **1990**, *24*, 9.
- (14) Ober, C. K.; Jin, J. I.; Lenz, R. W. *Adv. Polym. Sci.* **1984**, *59*, 130.
- (15) Jackson, W. J., Jr. *Mol. Cryst. Liq. Cryst.* **1989**, *169*, 23.
- (16) Ballauff, M. *Angew. Chem., Int. Ed. Engl.* **1989**, *28*, 253.
- (17) Noel, C. *Makromol. Chem., Macromol. Symp.* **1988**, *22*, 95.
- (18) Ungar, G.; Feijoo, J. L.; Keller, A.; Yourd, R.; Percec, V. *Macromolecules* **1990**, *23*, 3411.
- (19) Demus, D.; Richter, L. *Textures of Liquid Crystals*; Verlag Chemie; Weinheim, 1978.
- (20) Gray, G. W.; Goodby, J. W. *Smectic Liquid Crystals. Textures and Structures*; Leonard Hill: Glasgow and London, 1984.
- (21) Ungar, U.; Feijoo, J. L. *Mol. Cryst. Liq. Cryst.* **1990**, *180B*, 281.
- (22) Russell, T. P.; Koberstein, J. T. *J. Polym. Sci., Polym. Phys. Ed.* **1985**, *23*, 1109.
- (23) Robertson, J. M. *Proc. R. Soc.* **1935**, *A150*, 348.
- (24) Jeffrey, J. A. *Nature* **1945**, *156*, 82.
- (25) Bryan, R. F.; Hartley, P.; Miller, R. W.; Shen, M. S. *Mol. Cryst. Liq. Cryst.* **1980**, *62*, 281.
- (26) Bryan, R. F.; Hartley, P.; Miller, R. W. *Mol. Cryst. Liq. Cryst.* **1980**, *62*, 311.
- (27) Ungar, G.; Keller, A. *Mol. Cryst. Liq. Cryst.* **1988**, *155*, 313.
- (28) Boon, J.; Magre, E. P. *Makromol. Chem.* **1969**, *126*, 130.
- (29) Northolt, M. G. *Eur. Polym. J.* **1974**, *22*, 965.
- (30) Tabor, B. J.; Magre, E. P.; Boon, J. *Eur. Polym. J.* **1971**, *7*, 1127.
- (31) Fratini, A. V.; Cross, E. M.; Whitacker, R. B.; Adams, W. W. *Polymer* **1986**, *27*, 861.
- (32) Ungar, U. *J. Phys. Chem.* **1983**, *87*, 689.
- (33) Lueute, V.; Dollhopf, W. *Colloid Polym. Sci.* **1980**, *258*, 353.
- (34) Ungar, G.; Feijo, J. L.; Percec, V.; Yourd, R. *Macromolecules*, in press.
- (35) Pershan, P. S. *Structure of Liquid Crystal Phases. World Scientific Lecture Notes in Physics*; World Scientific: Teaneck, NJ, 1988, Vol. 23. Gray, G. W.; Goodby, J. W. *Smectic Liquid Crystals. Textures and Structures*; Heyden and Sone Inc.: Philadelphia, 1984; p 134.
- (36) Noel, C. In *Polymeric Liquid Crystals*; Blumstein, A., Ed.; Plenum: New York, 1985; Vol. 21.
- (37) Noel, C.; Friedrich, C.; Bosio, L.; Strazielle, C. *Polymer* **1984**, *25*, 1281.
- (38) Watanabe, J.; Hayashi, M. *Macromolecules* **1988**, *21*, 278.
- (39) Watanabe, J.; Hayashi, M. *Macromolecules* **1989**, *22*, 4083.

Registry No. BPE-10/12(1/1), 131489-64-0; BPE-8/12(1/1), 131236-56-1; desoxyanisoin, 120-44-5; (4-methoxyphenyl)acetic acid, 104-01-8; (4-methoxyphenyl)acetyl chloride, 4693-91-8; anisole, 100-66-3; 1,2-bis(4-methoxyphenyl)ethane, 1657-55-2; 1,2-bis(4-hydroxyphenyl)ethane, 6052-84-2.